Appendix

A. Proof of Equation (13)

As mentioned in Section 3.2 of the main paper, in order for the prototype-classifier learning paradigm to work well, the network is desired to have enough confident predictions for all classes to get robust $\hat{\mathbf{w}}_i^s$ and $\hat{\mathbf{w}}_i^t$. First, to promote the network to have diversified outputs, we propose to maximize the entropy of expected network prediction $\mathcal{H}(\mathbb{E}_{\mathbf{x}}[p(y|\mathbf{x};\theta)])$. Second, to get high-confident prediction for each sample, we perform entropy minimization on the network output. So the overall objective is:

$$\max \mathcal{H}(\mathbb{E}_{\mathbf{x}}[p(y|\mathbf{x};\theta)]) - \mathbb{E}_{\mathbf{x}}[\mathcal{H}(p(y|\mathbf{x};\theta))]. \tag{15}$$

Now we show that this objective equals maximizing the mutual information between input and output, *i.e.* $\mathcal{I}(y;\mathbf{x})$:

$$\begin{aligned}
&\mathcal{H}(\mathbb{E}_{\mathbf{x}}[p(y|\mathbf{x};\theta)]) - \mathbb{E}_{\mathbf{x}}[\mathcal{H}(p(y|\mathbf{x};\theta))] && (16)\\
=&\mathbb{E}_{\mathbf{x}}\left[\sum_{i=1}^{L} p(y_i|\mathbf{x}) \log p(y_i|\mathbf{x})\right] \\
&- \sum_{i=1}^{L} \mathbb{E}_{\mathbf{x}}[p(y_i|\mathbf{x})] \log \mathbb{E}_{\mathbf{x}}[p(y_i|\mathbf{x})]] && (17)\\
=&\mathbb{E}_{\mathbf{x}}\left[\sum_{i=1}^{L} p(y_i|\mathbf{x}) \log p(y_i|\mathbf{x})\right] \\
&- \mathbb{E}_{\mathbf{x}}\left[\sum_{i=1}^{L} p(y_i|\mathbf{x}) \log \mathbb{E}_{\mathbf{x}}[p(y_i|\mathbf{x})]\right] && (18)\\
=&\mathbb{E}_{\mathbf{x}}\left[\sum_{i=1}^{L} p(y_i|\mathbf{x}) \log \frac{p(y_i|\mathbf{x})}{\mathbb{E}_{\mathbf{x}}[p(y_i|\mathbf{x})]}\right] && (19)\\
=&\mathbb{E}_{\mathbf{x}}\left[\int p(y|\mathbf{x}) \log \frac{p(y|\mathbf{x})}{\mathbb{E}_{\mathbf{x}}[p(y|\mathbf{x})]}\, \mathrm{d}y\right] && (20)\\
=&\int p(\mathbf{x})\, \mathrm{d}\mathbf{x} \int p(y|\mathbf{x}) \log \frac{p(y|\mathbf{x})}{\int p(\mathbf{x}) p(y|\mathbf{x})\, \mathrm{d}\mathbf{x}}\, \mathrm{d}y && (21)\\
=&\int p(\mathbf{x})\, \mathrm{d}\mathbf{x} \int p(y|\mathbf{x}) \log \frac{p(y|\mathbf{x})}{p(y)}\, \mathrm{d}y && (22)\\
=&\iint p(y,\mathbf{x}) \log \frac{p(y,\mathbf{x})}{p(y)p(\mathbf{x})}\, \mathrm{d}y\, \mathrm{d}\mathbf{x} \;=\; \mathcal{I}(y;\mathbf{x}) && (23)
\end{aligned}$$

In addition, we estimate $\mathcal{H}(\mathbb{E}_{\mathbf{x}}[p(y|\mathbf{x};\theta)])$ with $\sum_{x\in\mathcal{D}} p(y|\mathbf{x};\theta) \log \hat{\mathbf{p}}_0$, where $\hat{\mathbf{p}}_0$ is a moving average of $p(y|\mathbf{x};\theta)$.

B. Additional Datasets Details

Overall statistics of the datasets and the number of labeled source examples used in our experiments can be found in Table 6. For Office [59], Office-Home [70] and VisDA [56], we follow the same setting in [39], randomly sampling labeled images from the source domain and ensure that each class has at least one labeled example. For DomainNet [55], we use the same split files as [60] and further select 1-shot and 3-shots labeled samples in the training set for each class.

C. Additional Implementation Details

We implemented our model in PyTorch [53]. We choose batch size of 64 for both source and target in self-supervised learning and batch size of 32 for the classification loss. The learning rate ratio between linear layer and convolution layer is set to $1:0.1$. We use SGD with weight decay rate $5e^{-4}$. For Office and Office-Home, we adaptively set temperature ϕ according to [41]. For VisDA and DomainNet, we fix ϕ to be 0.1 for more stable training. We set temperature τ to be 0.1 in all experiments. We choose hyper-parameters λ_{in} and $\lambda_{\text{cross}} \in \{1, 0.5\}$, and the weight $\lambda_{\text{mim}} \in \{0.05, 0.01\}$. As for parameters m (momentum for memory bank update) and M (number of k-means in $\mathcal{L}_{\text{InSelf}}$), we set $m = 0.5$ and $M = 20$.

We use spherical k-means for clustering and set half of the number of clusters in k-means to be the number of the classes n_c, and the rest to be $2n_c$. We compute the weight for cosine classifier only using source images for the first 5 epochs and set t_w to be around half of the average number of images per class. New prototypes (*i.e.* centroids of clusters and weights of cosine classifier) are computed per epoch for both self-supervised learning and classification.

D. Quantitative Feature Analysis

To quantitatively compare the quality of learned features with different approaches, we perform classification with weighted k-nearest neighbor (kNN) classifier proposed by Wu *et al.* [73] in a cross-domain manner. Specifically, given a test image $\mathbf{x}^t$, we first compute its normalized feature $\mathbf{f}^t = F(\mathbf{x}^t)$, and then compare it again embeddings of all source images in the source memory bank $\boldsymbol{V}^s$ using cosine similarity $s_i = \cos(\mathbf{f}^t, \mathbf{v}_i^s)$. The top k nearest neighbors in the source domain, $\mathcal{N}_k$, would be used to make the final prediction with weighted voting. Specifically, class c would get weight $w_c = \sum_{i\in\mathcal{N}_k} \alpha_i \cdot 1(c_i = c)$, in which α_i is the contributing weight of neighbor $\mathbf{v}_i^s$ defined as $\alpha_i = \exp(s_i/\tau)$. We set $\tau = 0.07$ and $k = 200$ as in [73].

We perform the above cross-domain kNN classification on models trained with 1) only cross-domain self-supervised learning methods, and 2) Few-shot Unsupervised Domain Adaptation methods, with the results shown in Table 7 and Table 8, respectively. From the results, we can see that both the proposed cross-domain prototypical self-supervised learning method and the whole PCS framework outperforms previous approaches.

Table 6: Dataset statistics and labeled source used

Dataset	Domain	# total image	# labeled images	# classes
Office [59]	Amazon (A)	2817	1-shot and 3-shots labeled source	31
	DSLR (D)	498		
	Webcam (W)	795		
Office-Home [70]	Art (Ar)	2427	3% and 6% labeled source	65
	Clipart (Cl)	4365		
	Product (Pr)	4439		
	Real (Rw)	4357		
VisDA [56]	Synthetic (Syn)	152K	0.1% and 1% labeled source	12
	Real (Rw)	55K		
DomainNet [55]	Clipart (C)	18703	1-shot and 3-shots labeled source	126
	Painting (P)	31502		
	Real (R)	70358		
	Sketch (S)	24582		

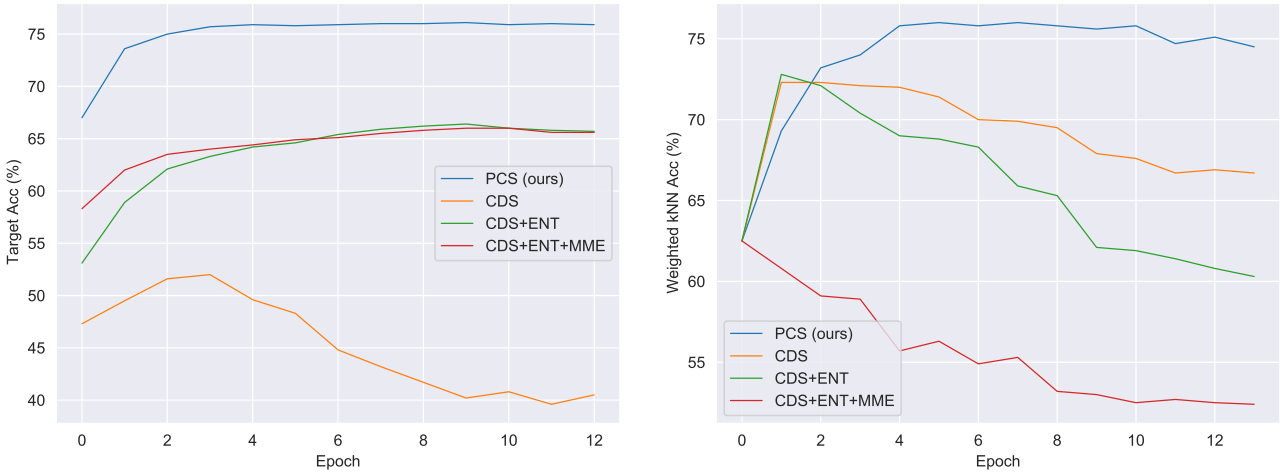

a Target Acc. with cosine classifier vs. training epochs

b Target Acc. with Weighted kNN vs. training epochs

Figure 6: Stability of Target Accuracy during training procedure.

Table 7: Accuracy of cross-domain weighted kNN with different SSL methods.

Method	D→A	Rw→Cl
ImageNet pre-train	62.5	40.6
ID [73]	70.3	51.9
CDS [39]	72.5	53.7
protoNCE [41]	72.3	49.3
$\mathcal{L}_{\text{InSelf}} + \mathcal{L}_{\text{CrossSelf}}$	**75.5**	**55.3**

Table 8: Accuracy of cross-domain weighted kNN with different FUDA methods.

Method	D→A (1-shot)	Rw→Cl (3%)
CDS [39]	72.3	57.6
CDS + ENT	72.8	58.6
CDS + MME + ENT	60.8	59.2
PCS (Ours)	**76.0**	**59.3**

E. Stability Analysis of PCS

To show the performance stability of PCS, we conduct multiple runs with three different random seeds. Table 9

Table 9: Averaged accuracy and standard deviation of PCS on three runs of 1-shot and 3-shots on Office dataset.

Labeled Source	A→D	A→W	D→A	D→W	W→A	W→D
1-shot	60.2±1.9	69.8±0.8	76.1±0.4	90.6±0.8	71.2±1.0	91.8±1.9
3-shots	78.2±1.8	82.9±1.1	76.4±0.5	94.1±0.1	76.3±0.7	96.0±0.7

Table 10: Sum of pair-wise cosine-similarity between prototypes in Office and Office-Home.

Method	D→A (1-shot)	Rw→Pr (3%)
SO	0.44	-0.71
CDS [39]	0.43	-0.71
PCS w/o APCU	-53.3	-22.8
PCS (Ours)	**-58.4**	**-26.5**

reports the averaged accuracy and standard deviation of the three runs on the 1-shot and 3-shots settings of Office.

Figure 6 shows adaptation accuracy vs. training epochs using cosine classifier (Figure 6a) and weighted kNN classifier (Figure 6b). From the plots, we can see that the target accuracy of PCS increases more steadily and robustly compared to other methods. In addition, PCS converges faster than other methods.

F. Prototype Quality Comparison

To further compare how well source and target are aligned, we provide more t-SNE [48] visualizations on Office (D→A) and Office-Home (Rw→Cl) in Figure 7a and 7b, comparing ImageNet Pre-training, CDS [39] and PCS. Specifically, we plot representations for all samples (top in both Figures), as well as the prototypes (normalized average representation) for each class. In top rows of both figures, the color of a sample represents its class, and samples from different domains are represented by different shapes (circles for source and crosses for target). In bottom rows of both figures, the number of a prototype represents its class index, and color represent the domain of the prototype (Cyan for source, Red for target, and Black for prototype weight of the classifier). As we can see from Figure 7, for each class, the prototypes of source, target and the weight vector of classifier gets more aggregated with PCS than other methods, which demonstrates that PCS could better align source and target domains.

In a well-learned feature embedding space, prototypes of different classes should be far / different from each other. To quantitatively measure the similarity of the learned prototypes, we compute the sum of cosine similarities between all pairs of prototypes. From the results shown in Table 10, we can see that the prototypes learned with PCS have the least similarities, indicating that PCS learns an embedding space with better semantic structure.

G. Image Retrieval Results

We present cross-domain image retrieval results in Figure 8. Given a query feature $\mathbf{f}_q$ in the target domain, we measure the pairwise cosine similarity between $\mathbf{f}_q$ and all features in the source domain. The source images with the most similar features as $\mathbf{f}_q$ are returned as the top retrieval results. We compare image retrieval results of PCS with CDS in Figure 8. In Figure 8, features from model trained with CDS are biased to some wrong color, texture and other visual clues; and quantitatively similar features do not correspond to semantically similar images in different domains. We can see that PCS could extract features that are more discriminative and semantically meaningful across domains.

H. Performance Comparison with UDA Methods using Full Source Labels

We have shown the superiority of PCS in label-scarce setting (FUDA), and we further conduct experiments with fully-labeled source domain (UDA). The performance comparison with other UDA methods on Office and Office-Home are presented in Table 12 and Table 11, respectively. We can see that PCS achieves the best results even with fully-labeled source, and this shows the proposed PCS could potentially be applied to a wide range of adaptation settings.

I. More Ablation Study Results

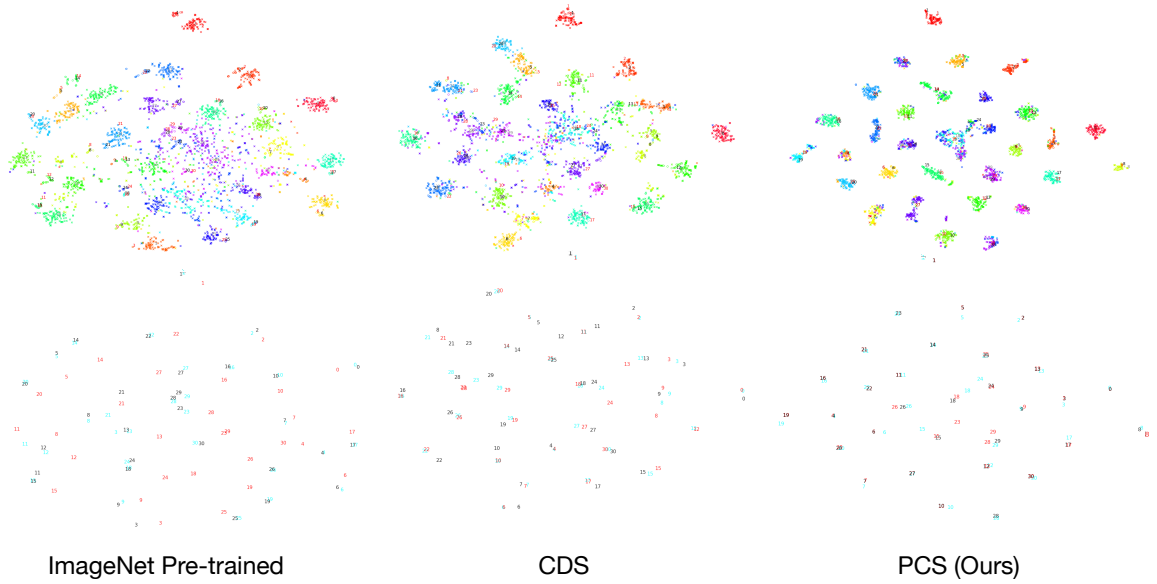

a Office (D→A with 1-shot labeled source per class)

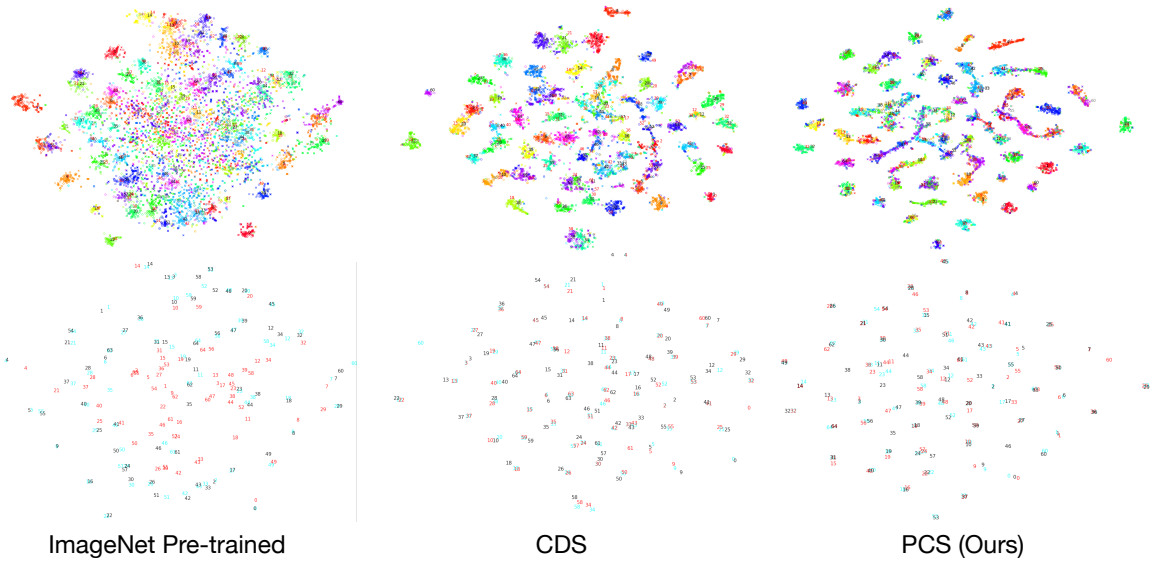

b Office-Home (Rw→Cl with 3% labeled source per class)

Figure 7: t-SNE visualization of ours and baselines on Office (a) and Office-Home (b). Top row: Coloring represents the class of each sample, and shape represents domain (circle for source and cross for target). Features with PCS are more discriminative than the ones with other methods. Bottom row: each number represents a centroid for corresponding class. **Cyan** represents centroids of source images based on ground truth and **Red** for target. **Black** represents prototypes of the classifier. Centroids from PCS are better-aligned between domains compared to other methods. (Zoom in for more details).

Table 11: Adaptation accuracy (%) comparison on fully-labeled setting on the Office-Home dataset.

Method	Ar→Cl	Ar→Pr	Ar→Rw	Cl→Ar	Cl→Pr	Cl→Rw	Pr→Ar	Pr→Cl	Pr→Rw	Rw→Ar	Rw→Cl	Rw→Pr	Avg
SO	34.9	50.0	58.0	37.4	41.9	46.2	38.5	31.2	60.4	53.9	41.2	59.9	46.1
DANN [18]	45.6	59.3	70.1	47.0	58.5	60.9	46.1	43.7	68.5	63.2	51.8	76.8	57.6
CDAN [45]	50.7	70.6	76.0	57.6	70.0	70.0	57.4	50.9	77.3	70.9	56.7	81.6	65.8
MMDIA [35]	56.2	77.9	79.2	64.4	73.1	74.4	64.2	54.2	79.9	71.2	58.1	83.1	69.5
MME [60]	54.2	72.8	78.3	57.9	70.2	71.8	58.5	52.9	77.9	72.7	58.1	81.8	67.3
CDS / MME [39]	56.9	73.3	76.5	62.8	73.1	71.1	63.0	57.9	79.4	72.5	62.5	83.0	69.3
PCS (Ours)	55.8	76.9	**80.3**	**67.9**	**74.0**	**75.7**	**67.0**	52.9	**81.0**	**74.5**	**58.3**	82.8	**70.6**

Figure 8: Image retrieval examples of the closest cross-domain neighbors using CDS (a) and PCS (b) in Office-Home (Target: Real, Source: Art).

Table 12: Adaptation accuracy (%) comparison on fully-labeled setting on the Office dataset.

Method	A→D	A→W	D→A	D→W	W→A	W→D	Avg
SO	68.9	68.4	62.5	96.7	60.7	99.3	76.1
DANN [18]	79.7	82	68.2	96.9	67.4	99.1	82.2
CDAN [45]	92.9	94.1	71	98.6	69.3	100	87.7
MMDIA [35]	92.1	90.3	75.3	98.7	74.9	99.8	88.8
MME [60]	88.8	87.3	69.2	98.7	65.6	100	84.9
CDS + MME [39]	86.9	88.3	75.9	98.6	73.3	100	87.1
PCS (Ours)	**94.6**	92.1	**77.4**	97.7	**77.0**	99.8	**89.8**

Table 13: Performance contribution of each part in PCS framework on Office-Home.

Method	Office-Home: Target Acc.												
	Ar →Cl	Ar →Pr	Ar →Rw	Cl →Ar	Cl →Pr	Cl →Rw	Pr →Ar	Pr →Cl	Pr →Rw	Rw →Ar	Rw →Cl	Rw →Pr	Avg
3% labeled source													
$\mathcal{L}_{\text{cls}}$	24.4	38.3	43.1	26.4	34.7	33.7	27.5	26.5	42.6	41.2	29.0	52.3	35.0
$+\mathcal{L}_{\text{InSelf}}$	34.6	48.3	54.7	49.2	53.1	57.1	48.2	40.6	62.9	57.9	44.9	68.8	51.7
$+\mathcal{L}_{\text{CrossSelf}}$	36.5	53.7	56.6	51.2	57.9	58.8	51.2	42.8	66.2	61.5	50.1	72.2	54.9
$+\mathcal{L}_{\text{MIM}}$	37.2	55.9	58.8	51.5	59.4	59.0	53.2	43.0	68.2	62.0	50.2	72.5	55.9
+APCU (PCS)	**42.1**	**61.5**	**63.9**	**52.3**	**61.5**	**61.4**	**58.0**	**47.6**	**73.9**	**66.0**	**52.5**	**75.6**	**59.7**
6% labeled source													
$\mathcal{L}_{\text{cls}}$	28.7	45.7	51.2	31.9	39.8	44.1	37.6	30.8	54.6	49.9	36.0	61.8	42.7
$+\mathcal{L}_{\text{InSelf}}$	40.8	57.6	65.5	54.5	62.4	62.7	54.6	43.1	73.6	64.2	44.7	75.9	58.3
$+\mathcal{L}_{\text{CrossSelf}}$	40.8	59.5	66.9	55.5	64.1	63.1	57.2	46.2	73.9	65.0	52.0	76.9	60.1
$+\mathcal{L}_{\text{MIM}}$	42.1	60.2	68.5	55.9	64.4	63.5	59.1	47.1	74.4	66.6	52.1	77.0	60.9
+APCU (PCS)	**46.1**	**65.7**	**69.2**	**57.1**	**64.7**	**66.2**	**61.4**	**47.9**	**75.2**	**67.0**	**53.9**	**76.6**	**62.6**